Efficiency of Waveguide Uni-Traveling-Carrier Photodiodes for Microwave Signal Generation

Brandon Isaac[1], Sergio Pinna[2], Yuan Liu[2], Jonathan Klamkin[2]
[1]*Materials Department, University of California, Santa Barbara, CA 93106*
[2]*Electrical and Computer Engineering Department, University of California, Santa Barbara, CA 93106*
Email: brandonjisaac@ucsb.edu

Abstract: The power conversion efficiency of uni-traveling-carrier photodiodes (UTC-PDs) and their limitations for generating microwave signals are discussed. The model is validated with experimental results from a fabricated waveguide UTC-PD that demonstrates a 60-GHz bandwidth.
OCIS codes: (040.5160) Photodetectors (130.0250) Optoelectronics

1. Introduction

Uni-traveling-carrier photodiodes (UTC-PDs) show promise for high-speed communication and generation of microwave and low THz signals. One promising application is W-band phased arrays using optical beam forming networks [1-3]. For this application, low loss SiN waveguide platforms can provide true time delay and efficient optical routing to provide squint free beam steering. UTC-PDs convert the optical signal to an electrical signal for driving the phased array antenna elements. UTC-PDs have potential for wide RF bandwidth and large output power compared to pin-PDs due to the faster transit time of the n-type carriers. UTC-PDs have a p-type absorbed which removes slower holes from transiting across the depletion region of the diode. This improves the bandwidth of the device and reduces the space-charge effect to improve RF output power saturation [4-6]. To date, researchers have demonstrated discrete UTC-PDs with bandwidths in excess of 100 GHz with RF output power of 7 dBm [7]. Furthermore, UTC-PDs integrated with antennas have demonstrated 3.5 μW, 28 μW, and 100 mW of detected power at 1.25 THz, 700 GHz, and 60 GHz respectively [8,9].

For microwave and sub-THz signal generation, the issue of power conversion efficiency is important for the utility of the technology. Compared to all electronic approaches or other photonic techniques to microwave signal generation, the UTC-PD based photomixing approach is widely tunable and is capable of large bandwidth. However, if the efficiency is not comparable, deployment in commercial applications may be limited. In one common implementation, UTC-PDs generate microwave signals by heterodyning two lasers and filtering the optical frequencies to produce an RF beat tone. Signals can be generated from the MHz to sub-THz regime provided the lasers are phase stabilized and the UTC-PD has sufficient bandwidth. However, as higher frequencies are approached, the photodiode design must balance responsivity, bandwidth, and RF output characteristics. This design trade-off can lead to very low overall power conversion efficiency. Here we discuss the power conversion efficiency and present experimental results to illustrate features of the power efficiency curve for 60 GHz UTC-PDs.

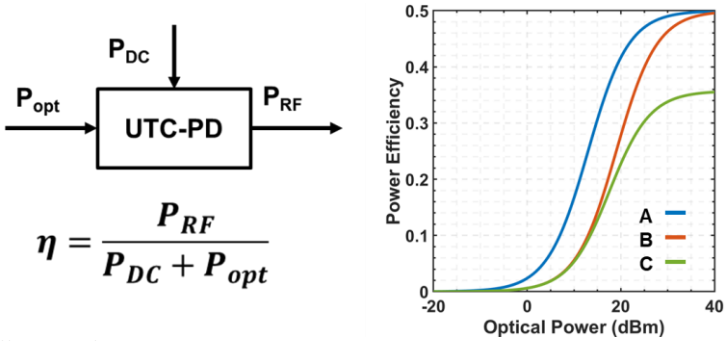

Figure 1 Power conversion efficiency of the optical-electrical conversion process. In the plot on the right, Curve A shows the efficiency of an ideal device with 0 Ω series resistance and responsivity of 1.24 A/W. Curve B shows the effect of reduced responsivity, while curve C shows the effect of series resistance and reduced responsivity.

The power conversion efficiency of a UTC-PD for a heterodyne setup is given by

$$\eta = \frac{P_{RF}}{P_{DC}+P_{opt}} = \left(\frac{2}{m^2\alpha R_L} + \frac{2\left(R_L+\frac{1}{\alpha}\right)}{mR_L} + \frac{2V_{th}}{m^2\mathcal{R}P_{opt}R_L} + \frac{2}{m^2\mathcal{R}^2P_{opt}R_L}\right)^{-1} \quad (1)$$

where m is the modulation index, α is the inverse of the device series resistance, R_L is the load impedance, $\mathcal{R}$ is the responsivity, and V_{th} is the bias to fully deplete the diode [10]. P_{DC} represents the power used to maintain the junction at a specific reverse bias, P_{opt} is the optical input power, and P_{RF} is the power deliver to a load (assumed 50 Ω here). From an efficiency perspective, P_{DC} can be optimized by adjusting the bias to be just below the onset of RF compression for a given photocurrent, which yields the second expression in equation 1.

As shown in Fig. 1, the power conversion efficiency is a non-linear function, which is due to the nature of the single photon to single electron conversion. One important feature, is that the efficiency approaches $\left(\frac{2}{m^2\alpha R_L} + \frac{2\left(R_L+\frac{1}{\alpha}\right)}{mR_L}\right)^{-1} \Rightarrow 50\%$ as the optical input power increases for an ideal device with 0 Ω series resistance ($\alpha \rightarrow \infty$) and 100% modulation index (curve A). However, series resistance, responsivity and modulation index affect the limiting value and power required to achieve the limiting value. Curve B illustrates the effect of reduced responsivity. A device with lower responsivity does not have a lower limiting efficiency; however, it requires higher optical powers to achieve the limiting value. Furthermore, this is not due to the higher optical power required to achieve the same RF power, but comes from the fourth term which is quadratic in the responsivity. This term is a result of the linear relation of the optical power with responsivity and the quadratic relationship with RF power. Curve C shows the effect of large series resistance in addition to reduced responsivity. Device series resistance lowers the limiting efficiency as a larger biasing voltage is required to maintain the same voltage drop across the device junction. In both cases, the ability to reach the limiting value is governed by the photodiodes ability to operate under high photocurrents and the reverse bias necessary to avoid RF compression at these photocurrents. We present a UTC-PD designed to achieve both high-RF output power and high bandwidth for microwave signal generation. The device is characterized to demonstrate the optical power dependence of the power conversion efficiency

2. Device Design and Fabrication

The mode simulation and epitaxial structure of the waveguide UTC-PD is shown in Fig. 2(a). An InGaAsP layer forms a passive waveguide, while an InGaAs layer provides a second absorbing, guiding layer. This two-layer waveguide structure allows for the integration with a spot size converter for more efficient coupling to SiN waveguide platforms for optical beam forming networks as mentioned earlier. The optical input contains only a passive waveguide using the InGaAsP layer. The InGaAs layer and thin InP depletion layer gradually taper from 500 nm to variable widths between 1 and 3 μm. The tapered waveguide input gradually brings the mode into the InGaAs layer and provides a more level absorption profile to achieve high RF output power. The higher RF output power is due to the reduced peak optically generated space charge in the device which leads to compression. The devices are fabricated by dry etching with methane-hydrogen-argon reactive ion etch down to the InP collector. A second dry etch defines the passive guiding layer. Photo-BCB is patterned to minimized parasitic pad capacitance, and finally P and N contacts are deposited. The fabricated device is shown in Fig. 2(b). The devices were thinned before cleaving to form facets for optical coupling. For the devices presented here, the optical facets formed do not form an efficient coupling to fiber, as no spot size converter was incorporated to simplify fabrication.

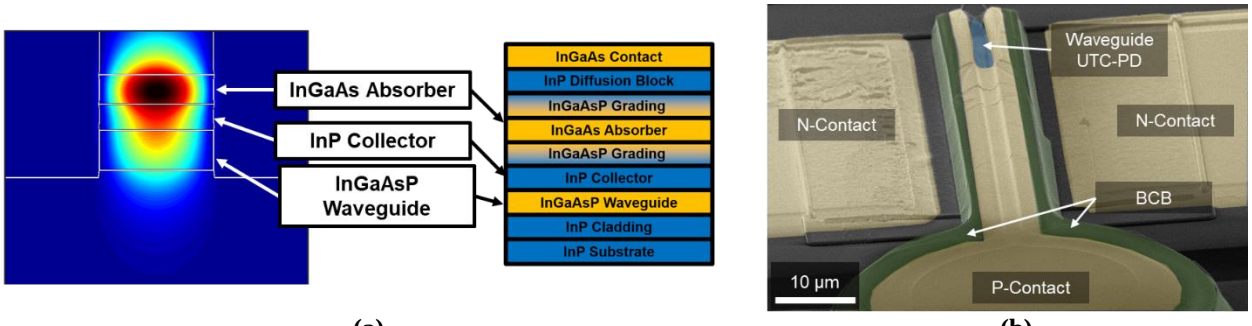

(a) **(b)**

Figure 2 (a) Mode simulation and epitaxial layers of the waveguide UTC-PD. (b) SEM of fabricated waveguide UTC-PD with faux coloring. The green highlights the low-k dielectric BCB that surrounds the PD ridge and lies under the P-contact to minimize parasitic capacitance. The blue highlights the active PD ridge, while the gold highlights the metals contacts.

3. Results and Discussion

The bandwidth of the fabricated devices ranges from 50 GHz to over 67 GHz. Two devices are shown in Fig. 3(a) demonstrating bandwidths of ~60 GHz at -3 V bias. Device B was used to demonstrate 30 Gb/s and 50 Gb/s non-return-to-zero (NRZ) on-off keying (OOK) data rates with open eyes as shown in Fig. 3(b). Measurements of the RF output power at 8 GHz were made on Device A shown in Fig. 3(b). At 0.5 V reverse bias, the device generated -6 dBm before the onset of compression. At higher reverse biases, the device generated over 6 dBm of RF output power. The data from the RF output power was used to generate the power conversion efficiency as a function of optical input power. The result is shown in Fig. 3(d) using equation 1. The sudden increase in the power conversion efficiency matches the theoretical curves shown in Fig. 1. The low power conversion efficiency can be attributed largely to the device responsivity being around 0.1 A/W. As mentioned above, the facets are not anti-reflection coated and the structure does not contain the spot size converter that the epitaxy layers were designed to include. The data from Fig. 3c can be used to extract each of the parameters used in expression 1, and generate a good fit of the data as shown by the dashed curve in Fig. 3d.

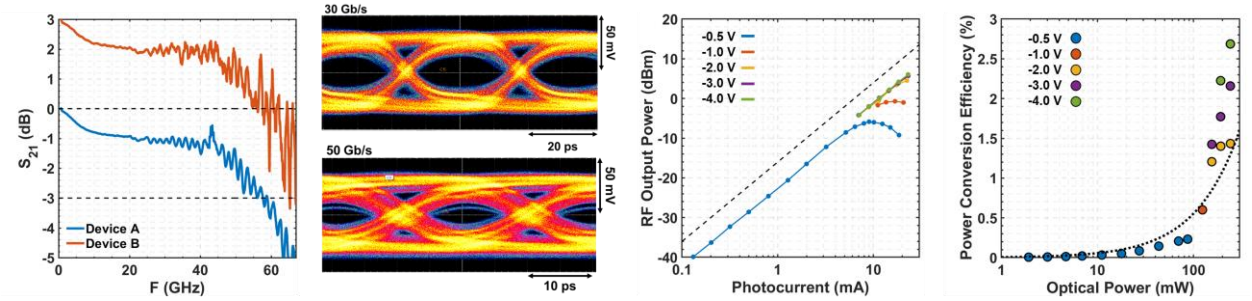

Figure 3 (a) Relative response of UTC-PD up to 67 GHz of two representative devices. (b) Eye diagram of Device B at 30 Gb/s and 50 Gb/s. (c) RF output power of Device A as a function of bias voltage at 8 GHz. Maximum RF output power measured reached 6 dBm. The black dashed curve is the ideal 50 Ω power curve. (d) Power conversion efficiency as a function of optical input power. Black dashed curve shows expression (1) plotted using parameters extracted from experimental data.

4. Conclusions

A waveguide UTC-PD was demonstrated with potential for microwave signal generation for optical beam forming networks. The power conversion efficiency was calculated and compared to the theoretical expression to demonstrate the non-linear conversion efficiency as the optical input power increases. The UTC-PD presented demonstrates a bandwidth of 60 GHz and clear eye openings up to 50 Gb/s. This work highlights the importance of designing PDs in order to obtain highly efficient power conversion for microwave signal generation.

5. Acknowledgements

The authors acknowledge support from the NASA Space Technology Mission Directorate (STMD) through an Early Stage Innovations (ESI) award. B. Isaac acknowledges funding from the NSF GFRP.

6. References

[1] Y. Liu et al, "Ultra-Low-Loss Silicon Nitride Optical Beamforming Network for Wideband Wireless Applications," JSTQE **24,** 1-10 (2018).
[2] Y. Liu, A. Wichman, B. Isaac, J. Kalkavage, E. Adles, T. Clark, and J. Klamkin, "Tuning Optimization of Ring Resonator Delays for Integrated Optical Beam Forming Networks," J. Lightwave Technol. **35**, 4954-4960 (2017).
[3] T. Nagatsuma, H. Ito, T. Ishibashi, "High-power RF photodiodes and their applications," Laser and Photonic Review **3**, 123-37 (2009)
[4] A. Beling et al. "InP-based waveguide photodiodes heterogeneously integrated on silicon-on-insulator for photonic microwave generation," Optics Express **21**, (2013)
[5] Z. Li et al. "High-Saturation-Current Modified Uni-Traveling-Carrier Photodiode with Cliff Layer," IEEE JQE **46**, (2010)
[6] Q. Li et al, "High-Power Flip-Chip Bonded Photodiode with 100 GHz Bandwidth," Journal of Lightwave Technology **34**, (2016)
[7] Q. Li et al. "High-Power Evanescently Coupled Waveguide MUTC Photodiode With >105-GHz Bandwidth," JLT **35**, (2017)
[8] [5] K. Li et al, "High-Power Photodiode Integrated with Coplanar Patch Antenna for 60 GHz Applications," IEEE Photonic Technology Letters **27, (**2015)
[9] H. Ito and T. Ishibashi "Terahertz-wave generation using resonant-antenna-integrated uni-traveling-carrier photodiodes," Proceedings of SPIE **10209**, 2017
[10] V. Urick, J. McKinney, and K. Williams, *Fundamentals of Microwave Photonics* (Wiley, 2018), Chap. 9.